

Cross section measurements for the $^{143}\text{Nd}(\text{n},\alpha)^{140}\text{Ce}$ reaction at 4.0, 5.0 and 6.0 MeV

Yu. M. Gledenov^a, M. V. Sedysheva^a, V. A. Stolupin^a, Guohui Zhang^b, Jiaguo Zhang^b,
Hao Wu^b, Jiaming Liu^b, Jinxiang Chen^b, G. Khuukhenkhuu^c, P. E. Koehler^d, P. J. Szalanski^e

^a *Frank Laboratory of Neutron Physics, JINR, Dubna 141980, Russia*

^b *State Key Laboratory of Nuclear Physics and Technology, Institute of Heavy Ion Physics,
Peking University, Beijing 100871, China*

^c *Nuclear research Centre, National University of Mongolia, Ulaanbaatar, Mongolia*

^d *Physics Division, Oak Ridge National Laboratory, Oak Ridge, Tennessee 37831, USA*

^e *University of Lodz, Institute of Physics, Lodz, Poland*

Abstract: Cross sections and forward/backward ratios for the $^{143}\text{Nd}(\text{n},\alpha)^{140}\text{Ce}$ reaction were measured at $E_n = 4.0, 5.0$ and 6.0 MeV using a twin-gridded ionization chamber and two large area back-to-back $^{143}\text{Nd}_2\text{O}_3$ samples. Experiments were performed at the 4.5 MV Van de Graaff of Peking University, China. Fast neutrons were produced through the $\text{D}(\text{d},\text{n})^3\text{He}$ reaction by using a deuterium gas target. A small ^{238}U fission chamber was employed for absolute neutron flux determination and a BF_3 long counter was as a neutron flux monitor. Present experimental data are compared with previous measurements, evaluations, and model calculations.

1. Introduction

Cross section data for the emission of charged particles following fast neutron bombardment are important for nuclear engineering applications as well as basic nuclear physics. Because the $^{143}\text{Nd}(\text{n},\alpha)^{140}\text{Ce}$ Q value is relatively large (9.722 MeV), the cross section for this reaction is measurable even at low energies; hence, several measurements have been made at thermal and resonance energies, as well as for 14-MeV neutrons [1,2,3,6,8,9,11,12]. In the MeV neutron energy region, however, there is only one datum, at $E_n = 3.0$ MeV, with large uncertainty [13]. As a result, there are very large differences between different evaluated nuclear data libraries such as ENDF/B-VII, ENDF/B-VI, JEFF3.1 and JENDL3.3 (ENDF, 2008). For example, at $E_n = 4.0$ MeV, the evaluated cross sections for $^{143}\text{Nd}(\text{n},\alpha)^{140}\text{Ce}$ are 0.70, 0.32, 0.032 and 0.60 mb, respectively, in the above mentioned four data libraries. To resolve these differences, cross section measurements in the MeV neutron energy region are needed for this reaction.

Measuring $^{143}\text{Nd}(\text{n},\alpha)^{140}\text{Ce}$ cross sections at MeV energies is difficult because both the cross section and available monoenergetic neutron flux are relatively small, and the backgrounds potentially large. Measurements are further limited by the fact that the samples must be relatively thin to reduce systematic uncertainties related to straggling of the outgoing α particles. Therefore, to obtain sufficient statistics, large area samples, α particle detector with high efficiency and large solid angle, and long measurement times are needed.

In the present work, the α -particle detector was a twin gridded ionization chamber containing two large area $^{143}\text{Nd}_2\text{O}_3$ samples. The detection efficiency and solid angle of the twin gridded ionization chamber are nearly 100% and 4π , respectively. Cross sections for the $^{143}\text{Nd}(\text{n}, \alpha)^{140}\text{Ce}$ reaction as well as forward/backward ratios for the emitted α particles (in the laboratory reference system) were measured at $E_n = 4.0, 5.0$ and 6.0 MeV. Because (n , charged particle) cross sections generally are lower for higher-Z materials, krypton was used instead of the more usual argon as the main working gas in the ionization chamber. Although the background was still relatively strong at lower charged-particle energies, α events from the $^{143}\text{Nd}(\text{n}, \alpha)^{140}\text{Ce}$ reaction could be separated from the background because the Q value of the measured reaction is large (9.722 MeV) compared to that of other reactions. Details of our experiment are illustrated in the next section followed by experimental results and discussions.

2. Details of experiment

Experiments were performed at the 4.5 MV Van de Graaff of Peking University, China. As shown in Fig.1, the setup of our experiment consisted of three main parts: the twin gridded ionization chamber, neutron source, and neutron flux detectors.

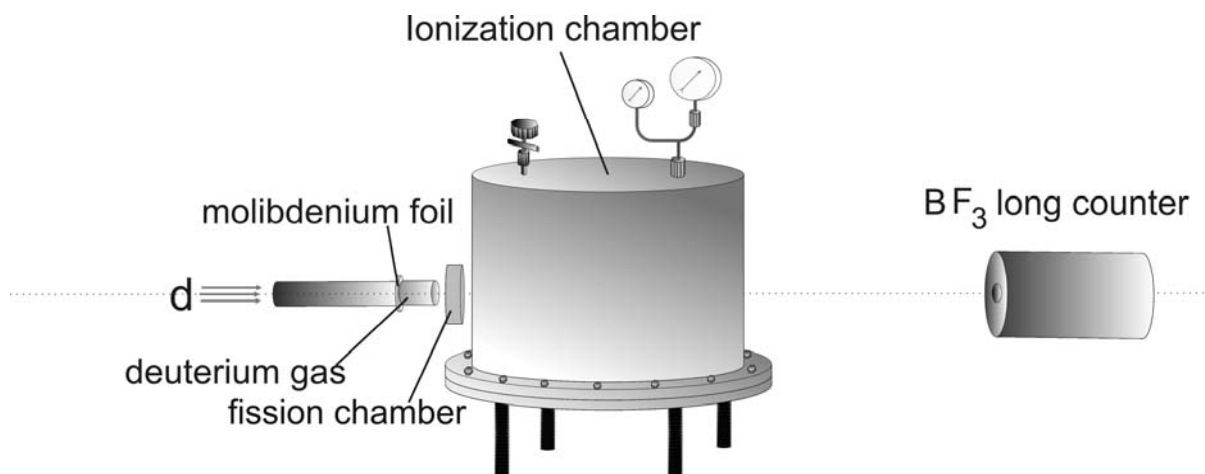


Fig. 1. Setup of the experiment.

The twin gridded ionization chamber (Fig.2), comprised of two symmetric sections with common cathode, was constructed at the Frank Laboratory of Neutron Physics, in Dubna, Russia. The outer wall of the chamber was an aluminum cylinder, 29.0 cm in height by 37.0 cm in diameter, with 2.0-mm thick walls. The cathode, grids, and anodes were rectangular. The grids consisted of parallel tungsten wires, coated with gold, which were 0.10 mm in diameter and spaced 2.0 mm apart. The effective grid area was $16 \times 18 \text{ cm}^2$. Distances from the cathode to grid and from the grid to anode were 75 and 20 mm, respectively.

A mixture of Kr + 2.89% CO₂ was used as the working gas for the ionization chamber. A gas pressure of 1.90 atm was used to ensure α particles from the $^{143}\text{Nd}(\text{n}, \alpha)^{140}\text{Ce}$ reaction were stopped before reaching the grids. The high voltages for the cathode, grid and anode were -3000, 0 and 1500 V, respectively, to allow complete collection of the electrons.

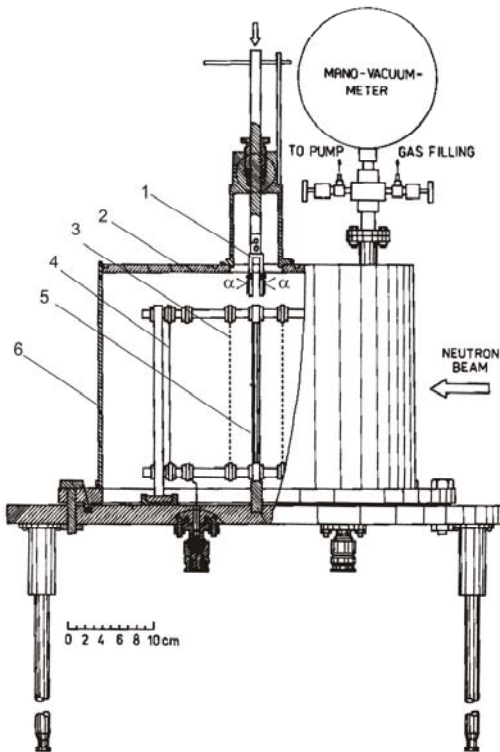


Fig. 2. Schematic view of the gridded ionization chamber

- 1 - α sources
- 2 - aluminum cover
- 3 - Frisch grids
- 4 - anode
- 5 - cathode
- 6 - aluminum cylinder 2 mm thick

The samples were $^{143}\text{Nd}_2\text{O}_3$ enriched to 83.5% in ^{143}Nd . The two samples were placed back to back, attached to the common cathode of the ionization chamber, and oriented perpendicular to the incident neutron beam. The samples were 4.077 and 3.875 mg/cm² thick for forward (0-90°) and backward (90-180°) α events, respectively, and the diameter of both samples was 10.8 cm. The backings of the samples were 0.005-in thick aluminum.

Two retractable α sources inside the gridded ionization chamber were used for energy calibration and adjustment of the data acquisition system.

Neutrons were produced through the D(d, n)³He reaction by using a deuterium gas target. The diameter and the length of the cylindrical gas cell were 0.9 cm and 2.0 cm, respectively. The gas cell was separated from the vacuum tube through a molybdenum foil 5.0 μm in thickness. The deuterium gas pressure was 2.9–3.1 atm during experiment. The energies of the accelerated deuteron beam before reaching the molybdenum foil were 1.79, 2.46 and 3.26 MeV, which according to Monte Carlo simulations, correspond to neutron energies of 4.0 ± 0.23 , 5.0 ± 0.16 and 6.0 ± 0.12 MeV respectively.

Absolute neutron flux was determined by a small parallel plate ^{238}U fission chamber positioned between the gridded ionization chamber and the gas target. The abundance of the ^{238}U sample was better than 99.997%. The mass of the ^{238}U sample was 547.2 ± 7.1 μg , the diameter was 2.0 cm. The working gas of the fission chamber was flowing Ar+2.85% CO₂ gas at a pressure slightly higher than 1.0 atm. A BF₃ long counter was used as a neutron flux monitor during the measurements.

The centers of the gridded ionization and fission chambers were at 0°, and the samples perpendicular to the incident neutron beam. The axis of the BF₃ long counter was also at 0° to the beam line. The distances from the center of the gas target to the ^{238}U and investigated samples were 3.45 and 35.5 cm, respectively.

The distance from the front side of the BF_3 long counter to the gas target was about 2.4 m. The intensity of deuteron beam was about 3.5 μA during measurement. Durations for $E_n = 4.0, 5.0$ and 6.0 MeV measurements were about 36, 22, and 19 h, respectively.

Two dimensional cathode versus anode spectra for both forward- and backward-emitted α particles were recorded simultaneously as illustrated in the block diagram of the electronics in Fig. 3. Anode spectra of the ^{238}U fission chamber also were recorded at the same time for absolute neutron flux determination.

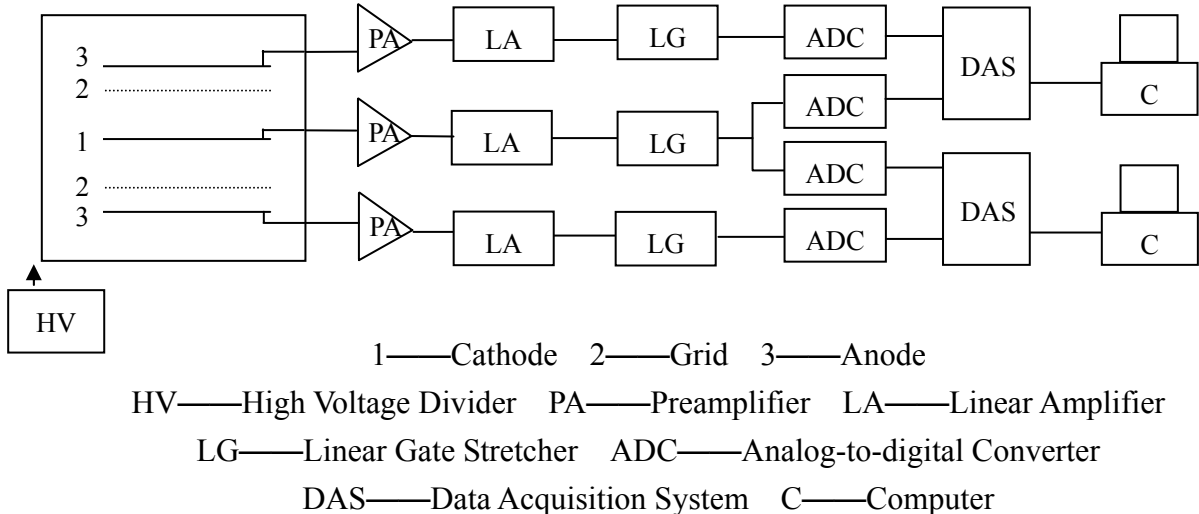


Fig. 3. Block diagrams of the electronics.

The $^{143}\text{Nd}(n, \alpha)^{140}\text{Ce}$ cross section σ_α was calculated using the following formula:

$$\sigma_\alpha = K \sigma_f \frac{N_\alpha}{N_f} \frac{N_{238U}}{N_{143Nd}} \quad (1)$$

where σ_f is the standard $^{238}\text{U}(n,f)$ cross section from ENDF/B-VII.0 library at the relevant energy; N_α and N_f are numbers of the α events from the $^{143}\text{Nd}(n,\alpha)^{140}\text{Ce}$ reaction and fission events from the $^{238}\text{U}(n,f)$ reaction, respectively; N_{238U} and N_{143Nd} are the atom numbers of ^{238}U and ^{143}Nd in the samples, respectively; and K is the neutron flux density ratio for ^{238}U and $^{143}\text{Nd}_2\text{O}_3$ samples. K was calculated numerically using the diameters of the samples and their distances to the gas target as well as the angular distributions of the $D(d, n)^3\text{He}$ reaction. The calculated values of K were 101.6, 96.7 and 92.5 for $E_n = 4.0, 5.0$ and 6.0 MeV , respectively, with relative uncertainty 3%.

3. Results and discussions

Fig.4 shows the forward direction cathode-anode two-dimensional spectrum for the $^{143}\text{Nd}(n,\alpha)^{140}\text{Ce}$ measurement at $E_n = 5.0 \text{ MeV}$. The area between the 0° and 90° curves [8] corresponds to the allowed region for α events from the $^{143}\text{Nd}(n,\alpha)^{140}\text{Ce}$ reaction. At lower anode channels, background from α events in the working gas obscures the signal of interest. The anode spectrum projected for events between the 0° and 90° lines in Fig.4 is shown in Fig. 5. Events from the $^{143}\text{Nd}(n, \alpha)^{140}\text{Ce}$ reaction are clearly seen as a peak near channel 150.

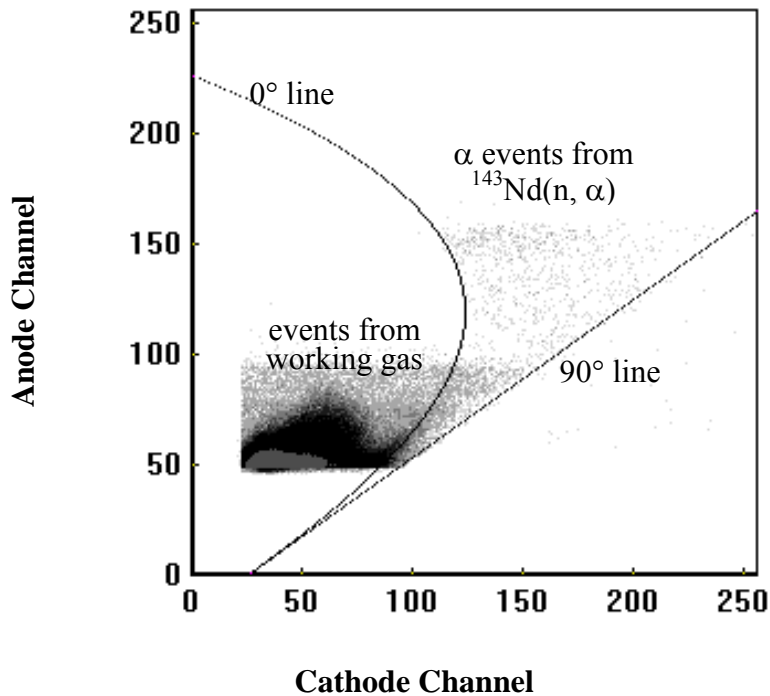


Fig. 4. Cathode-anode two-dimensional spectrum of forward events at $E_n = 5.0$ MeV.

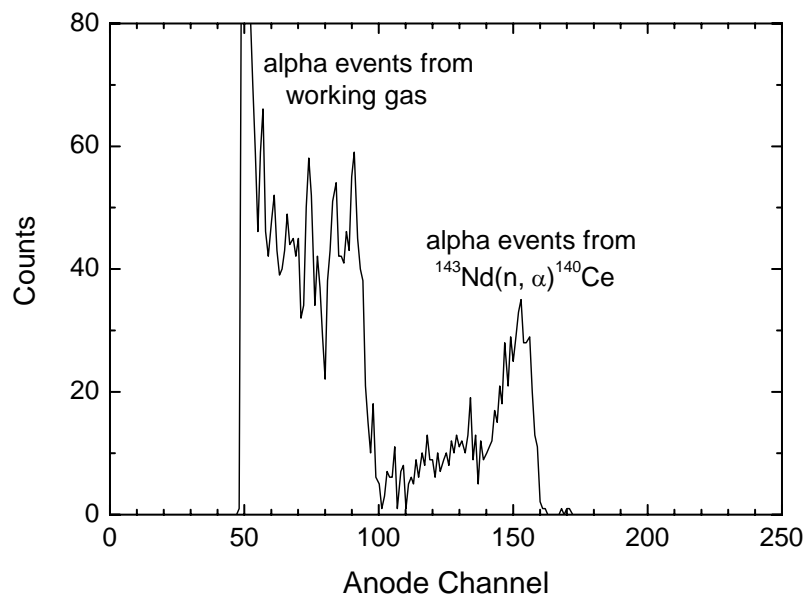


Fig. 5. Anode spectrum of forward events at $E_n = 5.0$ MeV between 0° line and 90° line.

The counts in this peak above threshold (channel 106 in Fig. 5) $N_{\alpha\text{det}}$ are less than the true number of counts N_α in formula (1) because, in addition to counts from the $^{143}\text{Nd}(n, \alpha)^{140}\text{Ce}$ reaction that are below threshold, some α particles are absorbed by the target.

The relationship between N_α and $N_{\alpha\text{det}}$ can be expressed as:

$$N_\alpha = \frac{N_{\alpha\text{det}}}{1 - R} \quad (2)$$

where R is much less than 1 in the present work. Values of R for the three incident neutron energies and the forward and backward direction data were estimated by Monte-Carlo simulations of α straggling in the sample, using the measured forward/backward α counting ratio. In estimating R , α energies corresponding to emission to the ground state of ^{140}Ce were used. Because this component is expected to dominate the cross section due to Coulomb barrier effects. From 4.0 MeV to 6.0 MeV, the estimated R value for forward alphas varied from 8.5% to 7.5%, and that for backward alphas from 12% to 18%. The uncertainty of R was estimated to be about 25%. Sources of uncertainties of $N_{\alpha\text{det}}$ include statistics (2.4–5%) and background subtraction (3–5%). Therefore, the uncertainty of N_α is (5–8.5%).

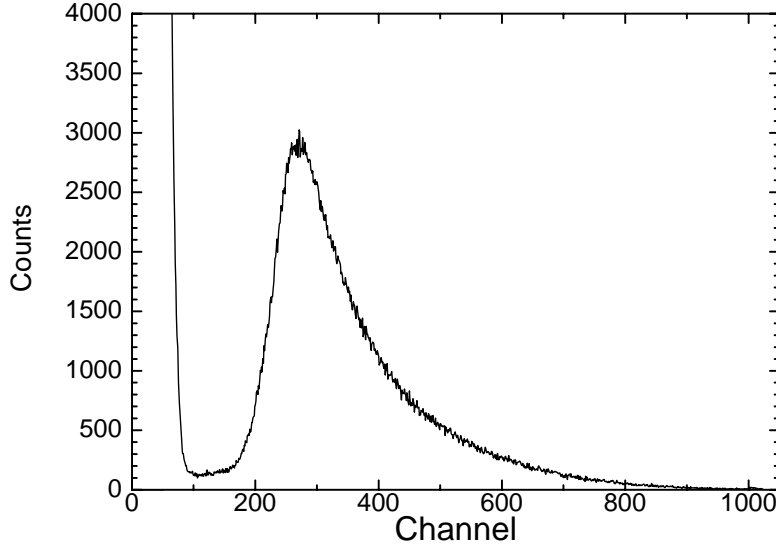


Fig. 6. Anode spectrum of the small ^{238}U fission chamber at $E_n = 5.0$ MeV.

Fig. 6 shows the anode spectrum from the small ^{238}U fission chamber for $E_n = 5.0$ MeV, from which the number of fission counts N_f was obtained.

The forward and backward cross sections were calculated using equation (1), and then added to get the total (n, α) cross section. The forward/backward cross section ratios depend only on the corrected numbers of forward and backward α events and the numbers of ^{143}Nd atoms in the two samples. Hence, the uncertainties in these ratios are not affected by uncertainties in K , σ_f , N_f , or N_{238U} in Equation 1.

In addition, the forward/backward cross section ratios were calculated. According to equation (1), the uncertainty of forward/backward cross section ratios are related only to the uncertainty of the forward and backward α events numbers N_α and the ^{143}Nd atom numbers $N_{143\text{Nd}}$.

The final cross sections also were corrected for attenuation of the neutron flux through the 2-mm thick aluminum wall of the ionization chamber. Using the total neutron cross section of aluminum in ENFD/B-VII, this correction factor was calculated to be 0.971, 0.972 and 0.975 for 4.0, 5.0 and 6.0 MeV neutrons, respectively. Also, the small difference in

average neutron energy in the $^{143}\text{Nd}_2\text{O}_3$ and ^{238}U samples was taken into account when using the standard $^{238}\text{U}(\text{n},\text{f})$ cross sections from ENDF/B-VII.0 library.

Cross sections and forward/backward ratios in the laboratory reference system for the $^{143}\text{Nd}(\text{n}, \alpha)^{140}\text{Ce}$ reaction are given in Table 1. The main source of uncertainty in the cross sections is due to uncertainties in the number of α events N_α (5–8.5%). Other sources of uncertainty include the neutron flux density ratio K (3%), fission counts N_f (2%), number of ^{143}Nd (1.5%) and ^{238}U (1.3%) sample atoms, and the ^{238}U fission cross section (1%). The total relative uncertainty is about 10%.

Our cross section data are compared with existing evaluations and experiments in Fig. 7. The cross section data at 12.3, 14.1 and 18.2 MeV were obtained by integration of the differential cross section data of Augustyniak et al. [6,7]. One can see from Fig. 7 that there are very large differences between different evaluations, especially in the region of the present measurements, and that no evaluation is consistent with all the available data.

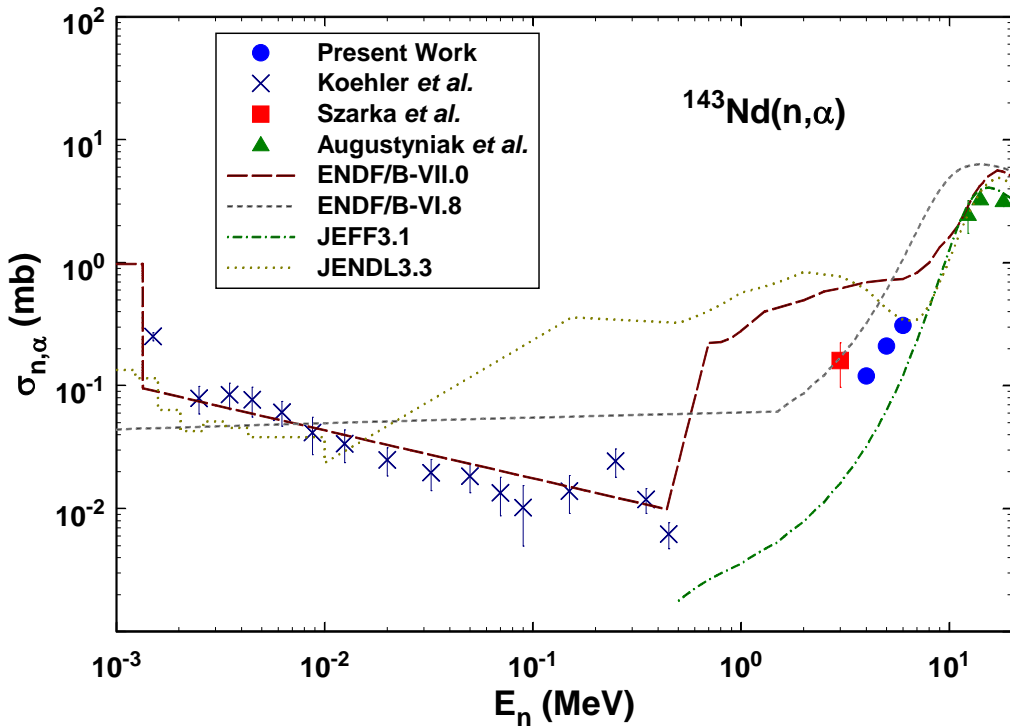


Fig. 7. Present cross sections compared with existing evaluations and measurements.

Table 1. Cross section data and forward/backward ratios in the laboratory reference system for the $^{143}\text{Nd}(\text{n}, \alpha)^{140}\text{Ce}$ reaction.

En (MeV)	$\sigma_{n,\alpha}$ (mb)	Forward/backward ratio
4.0 ± 0.23	0.12 ± 0.012	1.25 ± 0.12
5.0 ± 0.16	0.21 ± 0.021	1.78 ± 0.018
6.0 ± 0.12	0.31 ± 0.031	2.50 ± 0.025

Acknowledgements

This work was financially supported by the Russian Foundation for Basic Research (RFBR-NSFC 07-02-92104) and the National Natural Science Foundation of China (10875006, 10811120014) and China nuclear Data Center. The crew of the 4.5 MV Van de Graaff accelerator of Peking University is acknowledged for kind cooperation and support.

References

1. Andrzejewski Yu., Tkhan V. K., Vtyurin V. A., Koreivo A., Popov Yu. P., Stempinski M., 1980. Investigation of averaged cross-sections for (n, α) reactions on ^{123}Te , ^{143}Nd , ^{147}Sm and ^{149}Sm . Sov. J. Nucl. Phys. 32(6), 774-779.
2. Andrzejewski Yu., Vertebny V. P., Tkhan V. K., Vtyurin V. A., Kirilyuk A. L., Popov Yu. P., 1988. Study of (n, α) partial cross-sections on ^{143}Nd , ^{147}Sm , ^{149}Sm by filtered neutron beams. Yad. Phys. 48, 20-26.
3. Augustyniak W., Glowacka L., Jaskola M., Khoi L. V., Turkiewicz J., Zemlo L., 1983. Angular distributions of alpha particles from the $^{143}\text{Nd}(n, \alpha)^{140}\text{Ce}$ reaction induced by 12.3 , 14.1 and 18.2 MeV neutrons. INDC(POL)-012, 7-11.
4. Avrigeanu M., Avrigeanu V., 2009, α -particle optical potential tests below the Coulomb barrier, Phys. Rev. C 79, 027601-1 – 027601-4.
5. EXFOR: Experimental Nuclear Reaction Data, Database Version of December 19, 2008. url: <<http://www-nds.iaea.org/exfor/exfor.htm>>. Accession #30477002, 30477003 and 30477004.
6. Gadioli E., and Gadioli Erba E., Augustyniak W., Glowacka L., Jaskola M., Turkiewicz J., Dalmas J., 1988. Alpha-particle emission from fast-neutron-induced reactions on neodymium isotopes. Phys. Rev. C 38, 1649–1657.
7. ENDF: Evaluated Nuclear Data File, Database Version of January 16, 2009, url: <<http://www-nds.iaea.org/exfor/endf.htm>>.
8. Ito N, Baba M., Matsuyama S., Matsuyama I., Hirakawa N., 1994. Large solid angle spectrometer for the measurements of differential $(n, \text{charged-particle})$ cross sections, Nucl. Instr. Meth. A 337, 474-485.
9. Koehler P. E., Gledenov Yu. M., Andrzejewski J., Guber K. H., Raman S., Rauscher T., 2001. Improving explosive nucleosynthesis models via (n,α) measurements. Nuclear Physics A, 688(1-2), 86-89.
10. Koning A. J., Hilaire S., Duijvestijn M. C., 2008. TALYS-1.0., *Proceedings of the International Conference on Nuclear Data for Science and Technology - ND2007*, edited by O. Bersillon, F. Gunsing, E. Bauge, R. Jacqmin, and Sylvie Leray (EDP Sciences).
11. Okamoto K., 1970. The (n, α) Reaction on Samarium and Neodymium isotopes induced by thermal neutrons. Nucl.Phys. A141, 193–210.
12. Popov Yu.P., Salatski V.I., Khuukhenkhuu G., 1980. Averaged cross sections of the (n, α) reaction on ^{147}Sm , ^{143}Nd and ^{149}Sm in the neutron energy range 30 keV. Sov. J. Nucl. Phys. 32(4), 459-463.
13. Szarka I., Florek M., Jahn U., 1986. Gas proportional telescope used to investigate rare reactions induced by 3 MeV neutrons. Nucl. Instrum. Methods B 17, 472–474.